High speed nano-scale positioning using a piezoelectric tube actuator with active shunt control

S. Aphale, A.J. Fleming and S.O.R. Moheimani

Abstract: Piezoelectric tube scanners are the actuators of choice in scanning probe microscopy. These nanopositioners exhibit a dominant first resonant mode that is excited due to harmonics of the input scan signal. This introduces errors in the scan obtained. The presence of this resonant mode limits the upper bound of a triangular scan rate to around 1/100th of the first mechanical resonance frequency. Passive and active shunts have shown to damp this resonant mode substantially and improve scan performance. Sensorless active shunts optimised using H_2 and H_∞ techniques, is designed. These shunts reduce the amplitude of the first resonant peak of a prototype tube nanopositioner by 24 dB. A triangle wave input is used to test the improvement in scan performance due to the damping achieved by these active shunts. Analysis shows that damping the resonant mode in such fashion reduces the scan error by five times.

1 Introduction

Piezoelectric tube scanners were first reported in Binnig and Smith [1] for use in scanning tunnelling microscopes [2]. They were found to provide a higher positioning resolution and greater bandwidth than traditional tripod positioners while being simple enough to manufacture and easier to integrate into a microscope. Owing to their excellent displacement resolution, down to 10 pm, piezoelectric tube scanners are a key component in scanning probe microscopes [3], nanofabrication systems [4, 5] and nanomanipulation devices [6].

In many applications, piezoelectric tubes are designed with large length-to-diameter ratios; this provides a large deflection range but imposes low mechanical resonance frequencies. In nanometer precision raster scanning applications, such as SPM, the maximum triangular scan rate is limited to around 1/100th of the first resonance frequency of the tube. To illustrate the problem, consider a typical piezoelectric tube with maximum lateral deflection of 100 μm and a resonance frequency of 700 Hz. For an SPM, this equates to more than 60 s of image acquisition time (at VGA resolution) and severe throughput limitations in nanomanipulation and fabrication processes. The present work aims to damp the first lateral resonant mode and thus reduce the system response to external noise and induced vibration.

Feedforward and signal compensation approaches to vibration control have been studied extensively as their implementation requires no additional hardware or sensors and is noise efficient. It should be considered, however, that additional hardware such as displacement sensors and digital signal processors are required to identify the behaviour of each tube prior to implementation. In addition, although feedforward techniques do not add sensor noise to the control signal, they cannot provide any immunity to externally induced vibration. A technique for designing optimal linear feedforward compensators was presented in Croft *et al.* [7], then later extended to incorporate a PD feedback controller [8]. In these works, the authors identify the main limitation to performance as being modelling error. Other model-based feedforward approaches include [9, 10] and [11].

Feedback techniques can provide excellent low-frequency tracking performance but require an expensive and possibly difficult-to-integrate displacement sensor. Such techniques are most applicable to large scan ranges where sensor noise does not significantly degrade image quality, or at low speeds where the noise bandwidth can be significantly reduced. Good tracking of a 5 Hz triangle wave while maintaining robustness to non-linearity was presented in Salapaka *et al.* [12].

In Fleming *et al.* [13] a new vibration control technique, passive shunt damping, was applied to damp the first mechanical mode of a piezoelectric tube scanner. In this approach, an LRC impedance was connected to the piezoelectric transducer. When subject to deflection, the charge generated in the transducer flows through the external shunt impedance developing a counteractive voltage which can be optimised to result in significant vibration damping [14]. Shunt damping does not require a displacement sensor, is simple to implement and can be implemented with (essentially noise free) passive components. This paper extends the previous passive techniques to active and optimal shunt impedances that can damp a higher number of modes with greater performance.

2 Piezoelectric tube scanner

As shown in Fig. 1*b*, a piezoelectric tube scanner comprises of a hollow tube of radially poled piezoelectric material fixed at one end and free to deflect at the other. An electric

doi:10.1049/mnl:20065075

Paper first received 17th January 2007

The authors are with School of Electrical Engineering and Computer Science, University of Newcastle, Callaghan, NSW 2308 Australia

E-mail: sumeet.aphale@newcastle.edu.au

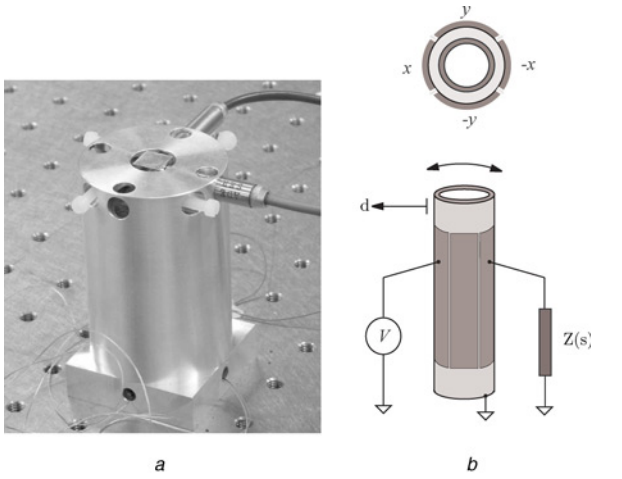

Fig. 1 *Piezoelectric tube scanner*

a Piezoelectric tube scanner with a cube mounted on top and placed in a protective aluminium cylinder that also acts as a socket for the capacitive sensors
b Internal construction of the piezoelectric tube scanner and a schematic of a shunt implementation
The inner electrode is grounded

field is generated within the actuator wall by four external electrodes and a grounded internal electrode. When a voltage is applied to one of the external electrodes, the actuator wall expands in a radial direction. Owing to Poisson coupling, the radial expansion causes a vertical contraction and large lateral deflection of the tube tip. Longer, narrower tubes of around 50–80 mm are used for achieving large deflections of around 100 μm, and shorter tubes of around 15 mm are used for small deflections of 1 μm or less.

Using the piezoelectric tube scanner as a nanopositioning platform in conjunction with a microcantilever, scans are obtained by moving either the piezoelectric tube scanner or micro-cantilever and keeping the other stationary. By tracing a raster-type pattern, where one axis receives a triangle wave input and the other a ramp input, the topology of the sample can be identified.

Owing to the small motion range, environmental noise can excite the resonant modes of a piezoelectric tube scanner. This is detrimental to the accuracy of the obtained scan. Thus, damping the first resonant mode of the piezoelectric tube scanner is extremely important. We describe a novel way of achieving this damping by implementing optimal sensorless shunts.

Small-deflection expressions for the lateral tip translation, derived from the IEEE Piezoelectricity Standard [15], can be found in Chen [16]. Measured in the same axis (x or y) as the applied voltage, the tip translation d is approximately

$$d_i = \frac{\sqrt{2}\, d_{31} L^2}{\pi D H} v_i \quad i = x, y \tag{1}$$

where d_i is the (x or y axis) deflection, d_{31} is the piezoelectric strain constant, L is the length of the tube, D is the outside diameter, h is the tube thickness and v_i is the (x or y axis) electrode voltage. Tip deflection can be doubled by applying an equal and opposite voltage to electrodes in the same axis. Vertical translation due to a voltage applied equally to all four quadrants is given approximately by

$$\Delta L = \frac{2 d_{31} L}{h} v \tag{2}$$

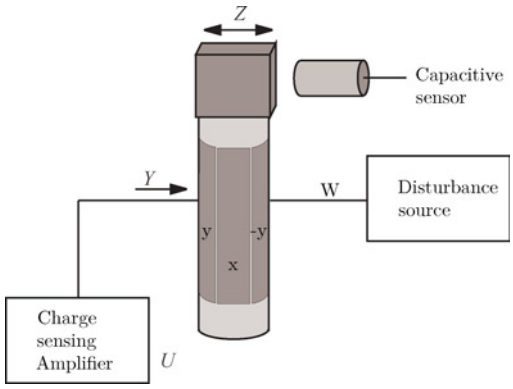

Fig. 2 *Schematic diagram denoting the inputs and outputs of the tube scanner*

3 System modelling and simulations

The piezoelectric nanopositioner is modelled as a two-input two-output system. The schematic experimental setup is shown in Fig. 2. $\boldsymbol{Z}$ and $\boldsymbol{Y}$ are the outputs, displacement and charge, respectively, and $\boldsymbol{W}$ and $\boldsymbol{U}$ are the inputs, disturbance and voltage. The charge is measured (in nano-coulombs) using a charge sensing amplifier and the displacement is measured (in micrometers) using a capacitive sensor. The frequency response function (FRF) $\boldsymbol{G}_{ij}(j\omega)$ is a 2×2 matrix where each element $\boldsymbol{G}_{ij}(j\omega), i,j = 1$ and 2, corresponds to a particular combination of the input and the output (for example $\boldsymbol{G}_{YW}(j\omega) = \boldsymbol{Y}(j\omega)/\boldsymbol{W}(j\omega)$ when $\boldsymbol{U} = 0$). These FRFs are determined by applying a sinusoidal chirp signal of varying frequency (from 10 Hz to 1 kHz) as input ($\boldsymbol{W}$ and $\boldsymbol{U}$) to the corresponding piezoelectric actuators and measuring the output signals ($\boldsymbol{Y}$ and $\boldsymbol{Z}$). As no dominant low frequency dynamics exist, this frequency range is suitable and captures the first resonant mode of the piezoelectric tube scanner. In a control theory setting, the system can be written in the standard matrix format

$$\begin{bmatrix} \boldsymbol{Z} \\ \boldsymbol{Y} \end{bmatrix} = \begin{bmatrix} \boldsymbol{G}_{zw}(s) & \boldsymbol{G}_{zu}(s) \\ \boldsymbol{G}_{yw}(s) & \boldsymbol{G}_{yu}(s) \end{bmatrix} \begin{bmatrix} \boldsymbol{W} \\ \boldsymbol{U} \end{bmatrix}$$

Using a subspace-based system identification technique [17], an accurate second-order model of the experimental system is obtained. Fig. 3 illustrates the measured two-input two-output frequency responses of the system as well as the identified model. The fit is simple and captures the system dynamics fairly accurately.

Once the four transfer functions are identified and modelled accurately, optimal shunt controllers are designed. To damp the piezoelectric nanopositioner, a regulator/controller for the transfer function between output charge and input voltage $\boldsymbol{G}_{\boldsymbol{YU}}$ that minimises a specific norm between input disturbance $\boldsymbol{W}$ and output displacement $\boldsymbol{Z}$ is needed. The principle behind shunt damping is to measure output charge $\boldsymbol{Y}$ and regulate input voltage $\boldsymbol{U}$ (the same principle that regulators work on) and thus, can be replaced by the controllers designed using H_2 and H_∞ optimisation techniques. Thus, optimal H_2 and H_∞ shunt controllers can be implemented synthetically for damping the low-frequency first resonant mode of the piezoelectric tube scanner. In order to design a shunt controller that is not of excessive gain, the performance output $\boldsymbol{Z}$ is augmented with the control signal multiplied by a weighting function [18]. In this work, H_2 and H_∞ optimisation techniques are used to design robust high performance shunts. These shunts are implemented using the dSPACE-DS1103 rapid prototyping system with a sampling frequency of 20 KHz.

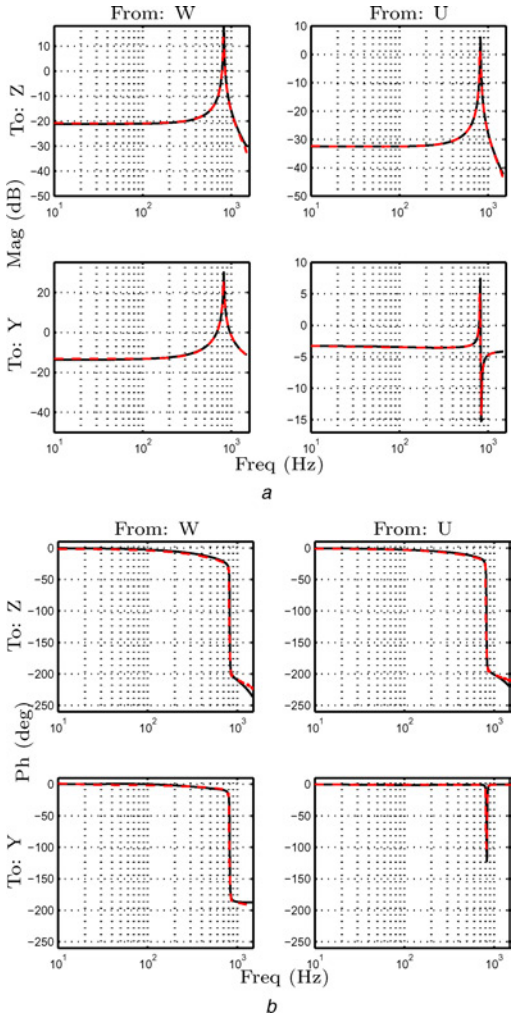

Fig. 3 *Magnitude and phase response of the actual (- -) and the modelled (—) tube nanopositioner system with inputs, disturbance (**W**) and voltage (**U**) and outputs, displacement (**Z**) and charge (**Y**).*
Note that the model captures the dynamics of the system with very high precision

Though two electrodes ($-y$ and y) are used in the experimental setup, it should be noted that only one of the electrodes is connected to the shunt and the other electrode is used to introduce a scanning waveform and to evaluate the damping performance. A penalty in using the damping network is that only one electrode can be used for scanning, thus, the scanning range is reduced by half.

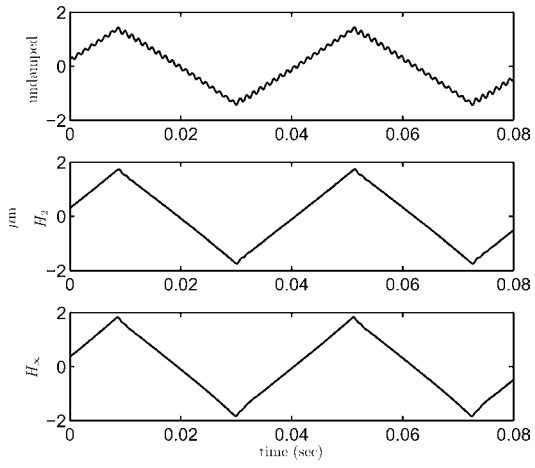

Fig. 4 *Triangle waveforms traced by the undamped tube scanner against the ones traced by the tube scanner damped using H_2 shunt and H_∞ shunt*

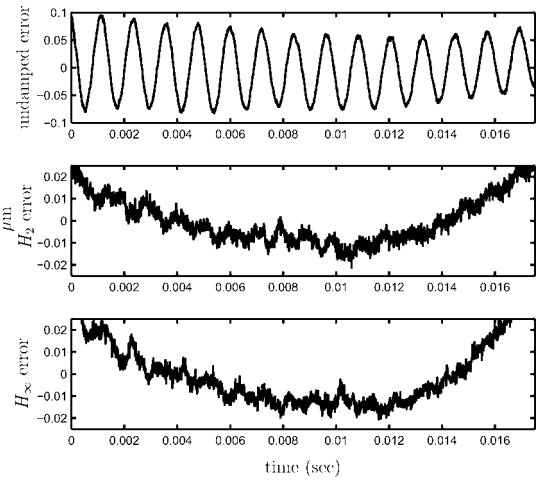

Fig. 5 *Plot of deviation from linear in 80% of scan waveform*
Note that the undamped deviation is plotted on a scale of ± 0.1 μm while the damped H_2 and H_∞ deviations are plotted on a scale of ± 0.02 μm

4 Experimental results

To evaluate the performance of the shunts designed, the piezoelectric tube scanner was made to trace a 16 Vpk,

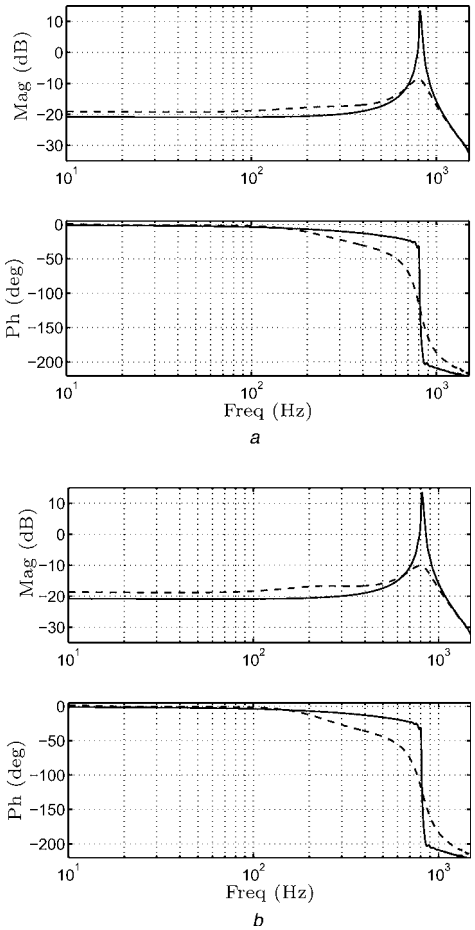

Fig. 6 *Undamped and damped transfer functions from the input disturbance **W** (in volts) to the output displacement **Z** (measured using a capacitive sensor with a gain of 0.1 V/μm)*
a Damping achieved by H_2 optimised shunt
b Damping achieved by H_∞ optimised shunt

Table 1: Errors in tracing the triangle wave

Type of system	Undamped	H_2 shunt controller	H_∞ shunt controller
Deviation from linear in 80% of scan waveform, nm	± 100	± 20	± 20

23.5 Hz triangle wave input [11]. The frequency response of the tube scanner exhibits a resonant peak at 814.6 Hz. The triangle wave input applied has harmonics which excite the first resonance and thus a clean triangle waveform is not traced. Fig. 4 shows the undamped and the damped triangle waveforms, traced by the tube scanner. The traced triangle (without any shunt damping) clearly shows the super-imposed high-frequency harmonics. H_2 and H_∞ shunts damp the resonant peak and thus the traced triangle waveform is cleaner, providing a more accurate scan of the sample of interest. Typical errors in tracing the triangle wave trajectory by the undamped and damped tube scanner with H_2 and H_∞ shunts are shown in Fig. 5.

An important benefit of the shunts so designed is that they do not need to be tuned, as they have a high performance spectrum and are virtually insensitive to slight variations in structural resonance frequencies. As can be seen from Fig. 6*a* and *b*, almost 24 dB of damping is achieved with the H_2 shunt and 25 dB of damping is achieved with the H_∞ shunt. As only one electrode is needed to implement the shunt, the need for an external sensor is completely eliminated.

5 Conclusions

The first resonant mode of a piezoelectric tube scanner has a significant effect on the scan accuracy. Active H_2 and H_∞ shunts can be designed with relative ease and they are capable of adding substantial damping to the dominant first resonant mode. As seen from Table 1, damping this resonant mode reduces the errors in the traced triangle wave by five times (from ± 100 to ± 20 nm). The shunts perform as per simulated predictions and 24–25 dB modal peak reduction is seen at the first resonant mode of the piezoelectric nanopositioner. The main contribution of this work lies in the total elimination of the sensor, which is necessary for implementing the previously known feedback control strategies. The penalty in sensorless shunt implementation is that the overall scan range is reduced by half. In this work, the capacitive sensor is used only to compare pre- and post-damping scan performance of the piezoelectric tube nanopositioner.

6 References

1 Binnig, G., and Smith, D.P.E.: 'Single-tube three-dimensional scanner for scanning tunneling microscopy', *Rev. Sci. Instrum.*, 1986, **57**, (8), pp. 1688–1689
2 Meyer, E., Hug, H.J., and Bennewitz, R.: 'Scanning probe microscopy' (Springer, Heidelberg, Germany, 2004)
3 Bonnell, D.A. redaktor: 'Scanning probe microscopy and spectroscopy – theory, techniques and applications' (John Wiley & Sons, 2001, 2nd edn.)
4 Tsenga, A.A., Notargiacomob, A., and Chen, T.P.: 'Nanofabrication by scanning probe microscope lithography: a review', *J. Vac. Sci. Technol.*, 2005, **23**, (3), pp. 877–894
5 Gates, B.D., Xu, Q., Love, J.C., Wolfe, D.B., and Whitesides, G.M.: 'Unconventional nanofabrication', *Ann. Rev. Mater. Res.*, 2004, **34**, pp. 339–372
6 Rubio-Sierra, F.J., Heckle, W.M., and Stark, R.W.: 'Nanomanipulation by atomic force microscopy', *Adv. Eng. Mater.*, 2005 **7**(4), pp. 193–196
7 Croft, D., McAllister, D., and Devasia, S.: 'High-speed scanning of piezo-probes for nano-fabrication', *Trans. ASME, J. Manuf. Sci. Technol.*, 1998, **120**, pp. 617–622
8 Croft, D., Stilson, S., and Devasia, S.: 'Optimal tracking of piezo-based nanopositioners', *Nanotechnol.*, 1999, **10**, pp. 201–208
9 Schitter, G., Stark, R.W., and Stemmer, A.: 'Fast contact-mode atomic force microscopy on biological specimens by model-based control', *Ultramicroscopy*, 2004, **100**, pp. 253–257
10 Schitter, G., and Stemmer, A.: 'Model-based signal conditioning for high-speed atomic force and friction force microscopy', *Microelectron. Eng.*, 2003, **67–68**, pp. 938–944
11 Perez, H., Zou, Q., and Devasia, S.: 'Design and control of optimal scan trajectories: Scanning tunneling microscope example', *J. Dyn. Sys. Meas. Control*, 2004, **126**, pp. 187–197
12 Salapaka, S., Sebastion, A., Cleveland, J.P., and Salapaka, M.V.: 'High bandwidth nano-positioner: A robust control approach', *Rev. Sci. Instrum.*, 2002, **75**, (9), pp. 3232–3241
13 Fleming, A.J., and Moheimani, S.O.R.: 'Sensorless vibration supression and scan compensation for piezoelectric tube nanopositioners', *IEEE Trans. Control Syst. Technol.*, 2006, **14**, (1), pp. 33–44
14 Fleming, A.J., and Moheimani, S.O.R.: 'Control oriented synthesis of high performance piezoelectric shunt impedances for structural vibration control', *IEEE Trans. Control Syst. Technol.*, 2005, **13**(1), pp. 98–112
15 Institute of Electrical and Electronics Engineers Inc. IEE standard on piezoelectricity: 'ANSI/IEEE Std. 176–1987', 1988.
16 Chen, C.J.: 'Electromechanical deflections of piezoelectric tubes with quartered electrodes', *Appl. Phys. Lett.*, 1992, **60**, (1), pp. 132–134
17 McKelvy, T., Akcay, H., and Ljung, L.: 'Subspace-based multivariable system identification from frequency-response data', *IEEE Trans. Autom. Control*, 1996, **41**, pp. 960–979
18 Doyle, J.C., Glover, K., Khargonekar, P., and Francis, B.: 'State-space solutions to standard H_2 and H_∞ control problems', *IEEE Trans. Autom. Control*, 1989, **34**, (8), pp. 831–847